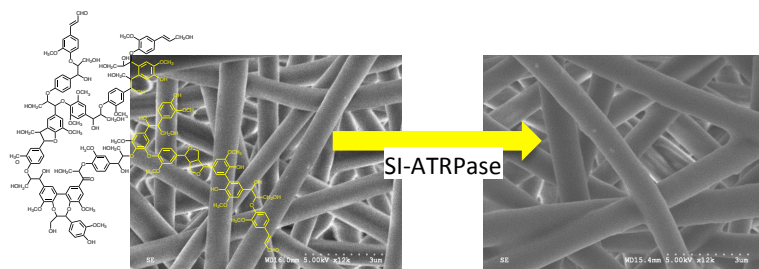




**Enzymatic Synthesis of Ionic Responsive Lignin Nanofibres
Through Surface Poly(N-isopropylacrylamide)
Immobilization**

Journal:	<i>Green Chemistry</i>
Manuscript ID:	GC-ART-04-2014-000757.R1
Article Type:	Paper
Date Submitted by the Author:	11-Jun-2014
Complete List of Authors:	Gao, Guangzheng; UBC, Karaaslan, Muzaffer; UBC, Kadla, John; NCSU, Ko, Frank; UBC,

TOC

Enzymatic Synthesis of Ionic Responsive Lignin Nanofibres Through Surface Poly(*N*-isopropylacrylamide) ImmobilizationGuangzheng Gao,¹ Muzaffer A. Karaaslan,¹ John F. Kadla*,² Frank Ko*¹¹Department of Materials Engineering, University of British Columbia, Vancouver, BC, Canada, V6T 1Z4²Department of Forest Biomaterials, North Carolina State University, Raleigh, NC, USA, 27695

Enzymatic Synthesis of Ionic Responsive Lignin Nanofibres Through Surface Poly(*N*-isopropylacrylamide) Immobilization

Guangzheng Gao,¹ Muzaffer A. Karaaslan,¹ John F. Kadla*,² Frank Ko*¹

¹Department of Materials Engineering, The University of British Columbia, Vancouver, BC, Canada, V6T 1Z4

²Department of Forest Biomaterials, North Carolina State University, Raleigh, NC, USA, 27695

Correspondence to:

John F. Kadla: jfkadla@ncsu.edu

Frank Ko: frank.ko@ubc.ca

Abstract:

Surface modification of electrospun lignin nanofibres with poly(N-isopropylacrylamide) (PNIPAM) was conducted through surface-initiated atom transfer radical polymerization (ATRPase) using various biocatalysts under aqueous conditions. Three biocatalysts were investigated, a catalase from bovine liver (CBL), a peroxidase from horseradish (HRP), and a laccase from *Trametes versicolor* (LTV). All of the biocatalysts were found to successfully graft PNIPAM polymer brushes from the nanofibre surfaces. PNIPAM brush thickness was dependent on enzyme activity and significantly influenced by the reaction conditions; manipulating the type of enzyme, the concentration of reducing reagent and solution pH resulted in PNIPAM brushes of various molecular weight, thickness, and grafting density. Lignin fibre surface immobilized PNIPAM brushes with a thickness of >100 nm and a corresponding molecular weight of more than 1×10^6 g/mole and a polydispersity index of less than 1.30 were obtained using LTV as the catalyst and ascorbic acid as the reducing agent. The effect of reducing reagent on the weight percentage of PNIPAM on the nanofibre surface was determined by measuring the enthalpy (ΔH) of the phase transition, which was found to exhibit a similar trend as that of the measured PNIPAM brush thickness. Finally, the low critical solution temperature (LCST) of PNIPAM immobilized lignin nanofibre was similar to that of pure PNIPAM and decreased with increasing the ionic concentration, which simultaneously changed the modified fibre mats from hydrophilic to hydrophobic.

KEYWORDS: Enzyme, ATRPase, PNIPAM, lignin, nanofibre, surface brush, LCST.

Introduction:

Lignin is one of the most abundant biomaterials in the world. However, its utilization for value-added products is limited to stabilizers, dispersants, and surfactants. This is primarily due to its role as an energy source for pulp and papermaking. As the need for renewable energy, chemicals and materials grows it will become increasingly important to extract more value from lignin. This will be particularly important as part of the evolving forest biorefinery.¹ Lignin-based fibres, particularly electrospun lignin nonwoven fibres, are one area of growing interest in both in academia and industry due their potential as precursors to carbon fibre and as well as novel functionalized materials. As a result our group has been focused on lignin-based value added novel products such as lignin micro- and nanofibres, carbon fibres,²⁻⁷ lignin-*co*-PNIPAM copolymers⁸ and environmental responsive lignin nanofibre mats via PNIPAM brush surface modification⁹.

Unlike most hydrophobic polymers used for the synthesis of micro- and nanofibers, lignins are quite unique. Lignins possess a number of different functional groups within their polymer backbone, which are amenable to functionalization and modification.^{1,3,8} This makes them ideal substrates for the design/development of novel surface functionalized fibrous materials, not readily achievable using traditional polymer systems. Surface modification through immobilization of polymer brushes is a very effective way to build new materials with novel functionalities.^{10,11} For example, surface immobilized PNIPAM, an amphiphilic stimuli-responsive polymer, offers temperature and ionic responsive surface properties to the modified substrate.^{12,13} Such surface modification of lignin-fibre mats may enable lignin utilization in applications, such as permeation-controlled filters,^{14,15} chemical sensors,¹⁶⁻¹⁸ attachment/detachment controllable surfaces for proteins^{19,20} and living cells,^{21,22} medical diagnostic devices,^{23,24} functional composite surfaces,²⁵ as well as thermo-reversible separators, thermo-responsive soft actuators, automatic gel valves, and smart, reusable catalysts.²⁶⁻³⁰

There have been many strategies for grafting polymer brushes on the surface of various materials. However, living radical polymer “grafting from” procedures have attracted considerable attention in recent years. In particular, surface-initiated atom transfer radical polymerization (**SI-ATRP**) has been widely studied for surface modification of solid materials such as fibrous structures.³¹

Enzymes are highly selective catalysts and key biomolecules involved in all *in vivo* metabolic reactions required to maintain “living life”. They are very specific and dramatically increase the rate of a reaction. As a result, biocatalysts have been extensively used in organic / polymer synthesis.³² Recently, a new enzyme catalyzed living controllable polymerization under aqueous conditions was discovered, ATRPase, which uses enzymes as the catalyst for atom transfer radical polymerization (ATRP).^{33,34} ATRPase using laccase from *Trametes versicolor* (LTV) as the catalyst was successfully used to immobilize poly(ethylene glycol) methyl ether methacrylate (PEGMA) polymer brushes onto the surface of crosslinked poly(styrene-2-hydroxyethyl methacrylate-divinylbenzene) particles (PSHMD).³⁵ Likewise, PNIPAM has been synthesized via ATRPase in a DMF/water solvent mixture using hematin as the catalyst.³⁶

Herein, for the first time, we demonstrated the enzymatic synthesis of PNIPAM polymer brushes immobilized on electrospun lignin nanofibre mats using a “grafting from” scheme under aqueous conditions at room temperature via SI-ATRPase. Three enzymes including a catalase from bovine liver (CBL), a peroxidase from horseradish (HRP), and a laccase from *Trametes versicolor* (LTV) were investigated and their effectiveness on the surface modification of lignin nanofibres with PNIPAM brushes is reported.

EXPERIMENTAL

Materials. *N*-Isopropylacrylamide (97%, Aldrich) was purified by recrystallizing from *n*-hexane prior to use. Water was purified using a Milli-Q Plus water purification system (Millipore Corp., Bedford, MA). Methanol and dichloromethane (DCM) were obtained from Fisher Scientific (Ottawa, ON) and used as received. Catalase from bovine liver (CBL, lyophilized powder, 2,000-5,000 units/mg protein, C9322), Peroxidase from horseradish (HRP, Type II, essentially salt-free, lyophilized powder, 150-250 units/mg solid (using pyrogallol), P8250), Laccase from *Trametes versicolor* (LTV, ≥ 10 U/mg, 51639), polyethylene oxide (PEO, $M_n = 1 \times 10^6$) were purchased from Sigma-Aldrich and used as received. Softwood Kraft lignin (Indulin AT) was obtained from Westvaco Corp. (Charleston, SC). It was washed with acidified water (pH = 2) five times before drying at 105 °C for 48 h. The dried material was then washed twice with methanol to remove low molecular mass material (dissolved roughly half of the lignin). The undissolved lignin was then air-dried overnight (12 h), ground with a mortar and pestle, and washed twice with a 70/30 (v/v) mixture of methanol/DCM (CH₃OH/CH₂Cl₂). The soluble fraction (30% of

the original lignin), herein referred to as SKL, was dried on a rotary evaporator at 50 °C and further dried on a Schlenk line at 100 mTorr, 60 °C. Phosphate buffered saline (PBS, pH = 7, 0.1 M) was prepared by monosodium phosphate and disodium phosphate. All other reagents were purchased from Aldrich and used as received.

Instrumentation. Attenuated total reflectance Fourier transform infrared (ATR-FTIR) spectra were recorded using a Perkin-Elmer Spectrum One FTIR spectrophotometer, 32 scans were acquired at a resolution of 4 cm⁻¹. Three different sites were tested for each sample, and the average value is reported.

Time dependent water contact angles were determined by placing a water droplet on the sample surface, and taking a series of pictures of the droplet at 2 s intervals using a digital camera (Retiga 1300, Qimaging Co.).

X-ray photoelectron spectroscopy (XPS) was performed using a Leybold LH Max 200 surface analysis system (Leybold, Cologne, Germany) operated with a Mg K α source, 200 W. Prior to XPS analysis, all samples were thoroughly dried under vacuum.

High resolution thermogravimetric analysis (TGA) was performed on a TA Instruments Q500 using approximately 3 mg of sample under nitrogen at a heating rate of 10 °C/min.

Phase transition temperatures were measured by differential scanning calorimetry (DSC, TA Instruments Q1000) using 2 mg samples with 10 μ L of water in hermetically sealed aluminum pans. The lower critical solution temperature (LCST) was determined by DSC.^{3,35} The samples were scanned at 2 °C/min over the temperature range of the phase transition from 5 to 50 °C, referenced against an empty pan. All temperatures were determined from the third heating scan.

SEM images were taken on Hitachi S3000N VP-SEM.

Polymer molecular weights were determined by gel permeation chromatography (GPC) on a Waters 2690 separation module fitted with a DAWN HELEOS multiangle laser light scattering (MALLS) detector from Wyatt Technology Corp (laser wavelength λ = 690 nm) and a refractive index detector (Optilab DSP) from Wyatt Technology Corp. operated at λ = 620 nm. The mobile phase was aqueous 0.1 N NaNO₃ at a flow rate of 0.8 mL/min. Aliquots of 200 μ L of the polymer solution were injected through two Waters Ultrahydrogel columns at 22 °C (guard column, Ultrahydrogel linear with bead size 6 – 13 μ m, elution range 10³ – 7 \times 10⁶ Da and Ultrahydrogel 120 with bead size 6 μ m, elution range 150 – 5 \times 10³ Da) connected in series. The

dn/dc value of PNIPAM in the mobile phase at 22 °C was determined at $\lambda = 620$ nm to be 0.164 mL/g and was used for molecular weight calculation.

^1H and ^{13}C NMR were measured using a Bruker Avance 300 MHz spectrometer. A total of 32 scans were acquired for ^1H NMR and 20K scans for ^{13}C NMR.

Lignin nanofibre mat preparation. Electrospinning of lignin was performed according to our previous report.³⁶¹⁹ The spinning dope was prepared by dissolving SKL (30 wt %) and PEO (0.2 wt %) in DMF at room temperature. Spinning was performed in a vertical orientation using an operating voltage of 15 kV, a solution flow rate of 0.03 mL/min, and a gap of 20 cm between the spinneret and collector. The as-spun fibre mats were then thermostabilized at a heating rate of 5 °C/min to 250 °C and held for 1 h to improve the mechanical performance of the fibres.

Surface initiator modification (SKL-Br). The lignin nanofibre surface ATRP-initiator was synthesized using a modified procedure of Gao et. al.⁹ Briefly, α -bromoisobutyryl bromide (1.00 mL, 8.1 mmol) was added dropwise over a period of 2 h to a lignin nanofibre mat (1×3 cm²) suspended in triethylamine (1.24 mL, 8.9 mmol) and DCM (40 mL) under stirring at 0 °C. The reaction was held at temperature for another 4 h, then allowed to warm to room temperature and left stirring overnight. The modified surfaces were cleaned twice by ultrasonication in DCM before being dried in vacuum. The dried ATRP initiator modified samples (Lignin-Br) were characterized using ATR-FTIR, TGA, SEM, XPS and water contact angle measurements.

Synthesis of PNIPAM brushes from SKL-Br by ATRPase. In a typical procedure NIPAM (0.8 g, 7.0 mmol) was dissolved in degassed water (4 mL) in a 10 mL Schlenk flask. Then L-ascorbic acid (AA) (0.1 g, 0.57 mmol) was added under argon, and the system was stirred until homogeneous. SKL-Br was introduced into the flask under argon and the solution was degassed by three cycles of freeze–pump–thawing. Then, LTV (20 mg) was added and polymerization was continued at room temperature for 24 h under argon and stirring. The polymerization was quenched by exposure air, followed by dilution with water. The resulting PNIPAM-grafted lignin fibre mats were then washed with water for 1 day, followed by methanol and DCM, respectively, and then dried in vacuum. The PNIPAM-grafted lignin fibre mat (LPN) was characterized by water contact angle measurements, SEM, XPS, ATR-FTIR, TGA and DSC analyses. Table 1 lists the various reaction conditions investigated.

Cleavage of PNIPAM Brushes. The grafted PNIPAM brushes were cleaved from the lignin nanofibre mats as described in literature.³⁶ The PNIPAM immobilized lignin fibre mat (LPN, $1 \times$

2 cm²) was put into 20 mL of 2 M NaOH aqueous solution, and reacted for 1 week at 50 °C. The resulting brown solution was removed from the reactor and the remaining insoluble PNIPAM was further dipped in 2 M NaOH aqueous solution to repeat the reaction two times. After removing the NaOH solution, PNIPAM was dissolved in water and neutralized with 0.1 M HCl followed by dialyzed for 2 days. The cleaved PNIPAM was obtained by freeze-drying and analyzed by NMR and GPC.

Table 1. Enzyme catalyzed lignin nanofibre surface PNIPAM brush grafting^a

sample ^b	solvent	reducing reagent	concentration of reducing reagent (×10 ⁵ , mol/L)	time (h)	M _n ^f (× 10 ⁴)	M _w /M _n ^f	Diameter ^j (nm)	Thickness ^l Δr (nm)	Grafting density ^k (ρ, chains/nm ²) (× 10 ²)
LPN-C-1	water	AA ^d	14.19	24	-- ^g	-- ^g	857 ± 87	14 ± 16	-- ^g
LPN-H-1	water	AA ^d	14.19	24	-- ^g	-- ^g	824 ± 85	~ 0	~0
LPN-L-1	water	AA ^d	14.19	24	56.67	1.23	963 ± 91	67 ± 21	8.40
LPN-C-2	water	AA ^d	5.68	24	21.54	1.53	907 ± 97	39 ± 27	12.39
LPN-H-2	water	AA ^d	5.68	24	7.84	1.66 ^h	850 ± 95	10 ± 25	8.55
LPN-L-2	water	AA ^d	5.68	24	74.34	1.40	1057 ± 87	113 ± 16	11.50
LPN-C-3	water	AA ^d	2.84	24	69.35	1.38	982 ± 96	87 ± 26	7.92
LPN-H-3	water	AA ^d	2.84	24	3.17	2.93 ⁱ	936 ± 92	53 ± 22	-- ^g
LPN-L-3	water	AA ^d	2.84	24	101.12	1.29	1029 ± 116	100 ± 42	7.30
LPN-C-4	water	AA ^d	1.42	24	72.97	1.31	1012 ± 94	99 ± 24	9.18
LPN-H-4	water	AA ^d	1.42	24	9.22	1.71 ^h	854 ± 84	12 ± 23	8.75
LPN-L-4	water	AA ^d	1.42	24	65.54	1.36	974 ± 89	72 ± 19	7.91
LPN-C-5	water	GL ^e	14.19	24	42.20	1.51	879 ± 84	25 ± 11	3.96
LPN-H-5	water	GL ^e	14.19	24	-- ^g	-- ^g	836 ± 83	~0	~0
LPN-L-5	water	GL ^e	14.19	24	-- ^g	-- ^g	828 ± 79	~0	~0
LPN-C-6	PBS ^c	AA ^d	5.68	24	-- ^g	-- ^g	862 ± 91	16 ± 21	-- ^g
LPN-H-6	PBS ^c	AA ^d	5.68	24	23.36	1.53	892 ± 86	31 ± 14	9.10
LPN-L-6	PBS ^c	AA ^d	5.68	24	21.39	1.50	870 ± 85	20 ± 13	6.34
LPN-C-7	water	AA ^d	0	24	-- ^g	-- ^g	821 ± 77	~0	~0
LPN-H-7	water	AA ^d	0	24	-- ^g	-- ^g	819 ± 85	~0	~0
LPN-L-7	water	AA ^d	0	24	-- ^g	-- ^g	835 ± 83	~0	~0

^a Condition: time: 24 h, diameter of lignin-Br: 830 ± 81 nm, NIPAM: 7 mmol, enzyme: 20 mg, solvent: 4 mL, at r.t..

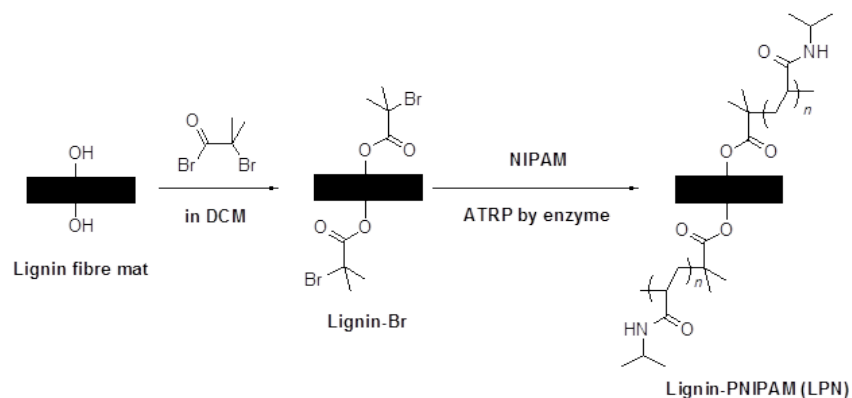
^b Catalyst: LPN-C: CBL, LPN-H: HRP, LPN-L: LTV. ^c pH: 6.0. ^d L-ascorbic acid. ^e α-D-glucose. ^f Determined by GPC. ^g Not determined. ^h Shoulder peak. ⁱ Multimodal. ^j Determined by SEM. ^k Calculated by equation 2.

RESULTS AND DISCUSSION

Lignin is known to have numerous reactive hydroxyl groups, which makes the surface of lignin nanofibre mats readily available to create active initiating sites for controlled polymerization reactions.

ATRP initiator immobilization on lignin nanofiber surface (SKL-Br). **Scheme 1** shows the synthetic procedure employed to modify the lignin nanofibres with the ATRP initiator. ATR-FTIR (**Figure 1**) and X-ray photoelectron spectroscopy (XPS) (**Figure 2**) analyses of the macroinitiator-immobilized surfaces clearly showed the incorporation of α -bromoisobutyryl moieties. Compared with the unmodified lignin nanofibre mat, the ATR-FTIR spectrum of the SKL-Br (**Figure 1B**) showed the carbonyl (C=O) stretching vibrations at 1760 cm^{-1} , consistent with α -bromoisobutyryl modification. In comparison to the unmodified lignin nanofibre, the surface-modified ATRP initiator sample, SKL-Br had three new small peaks at 250.7, 177.8, and 64.9 eV, corresponding to the Br 3s, Br 3p and Br 3d peaks of the α -bromoisobutyryl groups, respectively (**Figure 2**).

Scheme 1



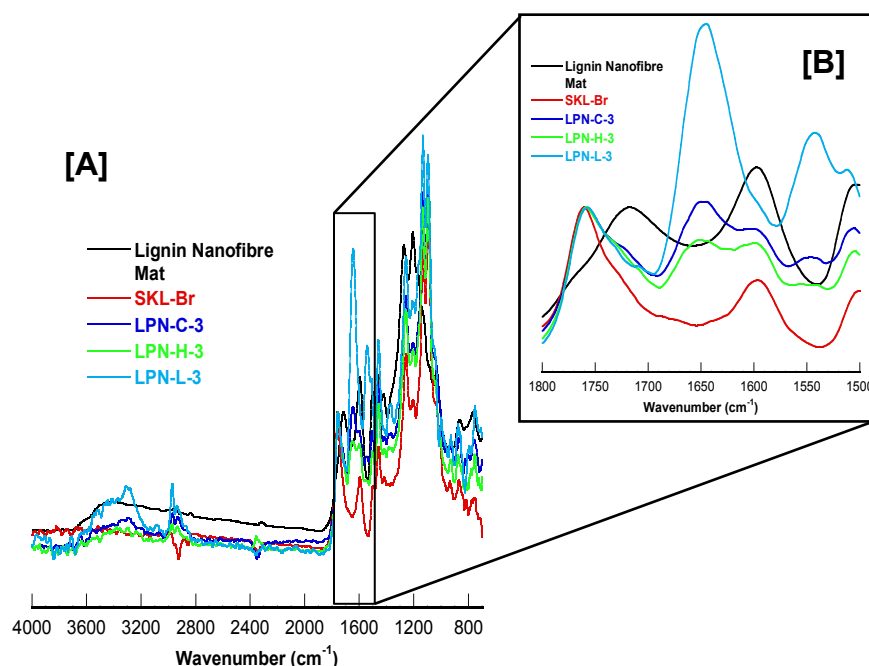


Figure 1. ATR-FTIR spectra of lignin nanofibre mats before and after enzyme catalyzed surface PNIPAM modification. **[A]:** ATR-FTIR spectra of a lignin nanofiber mat, lignin fiber initiator (SKL-Br) and PNIPAM modified lignin nanofibres catalyzed with CBL, HRP and LTV (samples in **Table 1**). **[B]:** ATR-FTIR spectra comparison of the typical signals at the wavenumbers of 1800 – 1500 cm^{-1} .

Enzymatically Catalyzed Synthesis of PNIPAM Brushes on the Lignin Nanofibre Surface. In this study, PNIPAM chains were “grafted from” the initiator immobilized lignin nanofibre surface for the first time by enzymatically catalyzed surface initiated ATRP (SI-ATRPase) under aqueous conditions. A series PNIPAM brush modified lignin nanofibre mats (LPNs) were synthesized by varying the type of enzyme (CBL, HRP and LTV), type and concentration of the reducing reagent and pH of the reaction medium (**Table 1**). SI-ATRPase resulted in the appearance of new peaks in the FTIR spectrum for all of LPN samples, corresponding to the amide stretching ($\nu_{\text{C=O}} \sim 1645 \text{ cm}^{-1}$; $\nu_{\text{N-H}} \sim 3300 \text{ cm}^{-1}$) and bending ($\delta_{\text{N-H}} \sim 1546 \text{ cm}^{-1}$) bands of the surface grafted PNIPAM (**Figure 1**). The height ratio of the amide stretching band ($\nu_{\text{C=O}} \sim 1645 \text{ cm}^{-1}$) to the SKL-Br initiator ester stretching band ($\nu_{\text{C=O}} \sim 1760 \text{ cm}^{-1}$) and the signal intensity at ~ 1645 and $\sim 1546 \text{ cm}^{-1}$ were related to the enzyme catalyzing activity and differed depending on the type of enzyme used (**Figure 1B**). For example, LPN-L-3 showed the strongest signal intensity at ~ 1645 and $\sim 1546 \text{ cm}^{-1}$ suggesting that the LTV resulted in a higher surface PNIPAM thickness as compared to that of CBL and HRP under the same conditions.

Successful PNIPAM grafting from the lignin nanofibre mat surface was confirmed by XPS analysis. The XPS spectra of the unmodified lignin nanofibre mats, after initiator immobilization (SKL-Br) and PNIPAM grafting are shown in **Figure 2**. It can be seen that the Br3s, Br3p and Br3d peaks of the SKL-Br disappeared and a new N1s peak at 399.4 eV appeared upon reaction with NIPAM, indicated the immobilization of PNIPAM polymer brushes onto the lignin nanofibre surface.

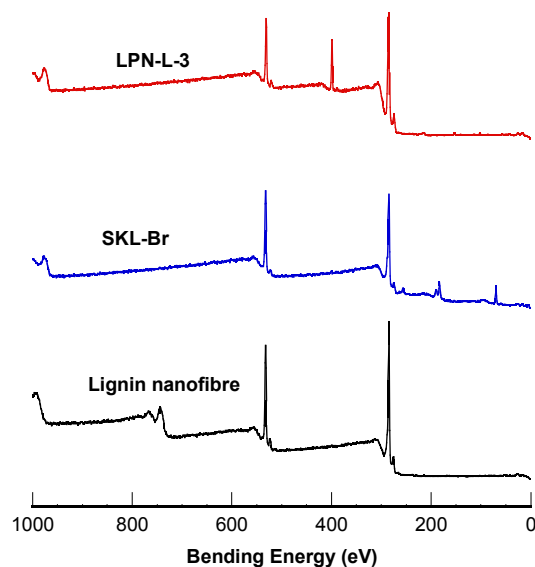


Figure 2. XPS spectra of lignin nanofibre mats; unmodified, initiator-immobilized (SKL-Br) and PNIPAM grafted.

Thermal gravimetric analysis (TGA) further showed the success of PNIPAM grafting onto the lignin nanofibre surface. The residual weight at 600 °C for LPN-L-3 was about 39.15 wt % as compared to about 44.19 wt % for the SKL-Br (**Figure 3**). Moreover, the LPN-L-3 thermogram shows two distinct decomposition profiles. The first, at ~250 °C is in good agreement with that of our previously reported lignin-g-NIPAM copolymers (252 °C) and that associated with certain lignin structures.⁸ The second onset of decomposition at ~400 °C is in good agreement with that of pure PNIPAM. The difference in the residual weight between LPN-L-3 and SKL-Br is about 5 %, which corresponds well with the DSC enthalpy results of the surface immobilized PNIPAM (*vide infra*).

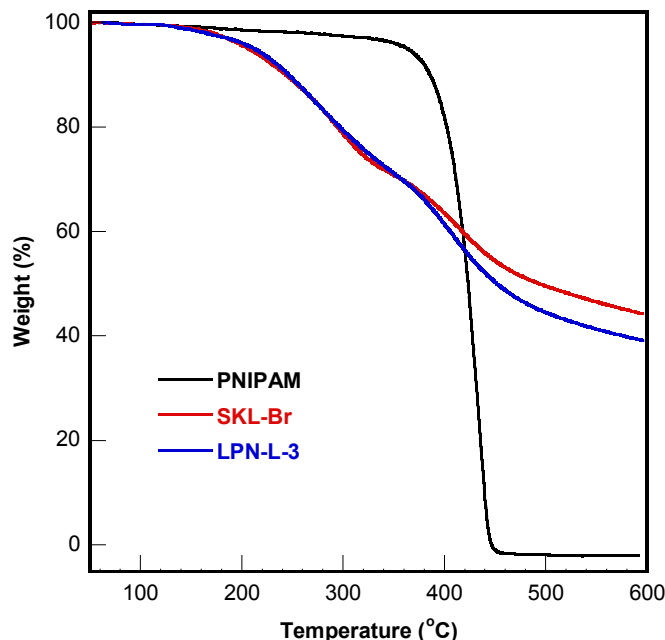


Figure 3. TGA traces of pure PNIPAM; initiator-immobilized (SKL-Br) and PNIPAM grafted lignin nanofibre mats (LPN-L-3).

SEM images of the lignin nanofibre mats before (SKL-Br) and after (LPN-L-3) SI-ATRPase are shown in **Figure 4**, and the fibre diameters under various reaction conditions are summarized in **Table 1**. The average diameter of the lignin nanofibres clearly increased after SI-ATRPase. The calculated thickness of the grafted PNIPAM layer was in the range from ~15 nm to ~110 nm; strongly related to the type of enzyme, the type and concentration of the reducing reagent, and solution pH. For example, at an AA concentration of 5.68×10^{-5} mol/L, the grafted brush thicknesses were 10 ± 25 , 39 ± 27 and 113 ± 16 nm for HRP, CBL, and LTV, respectively.

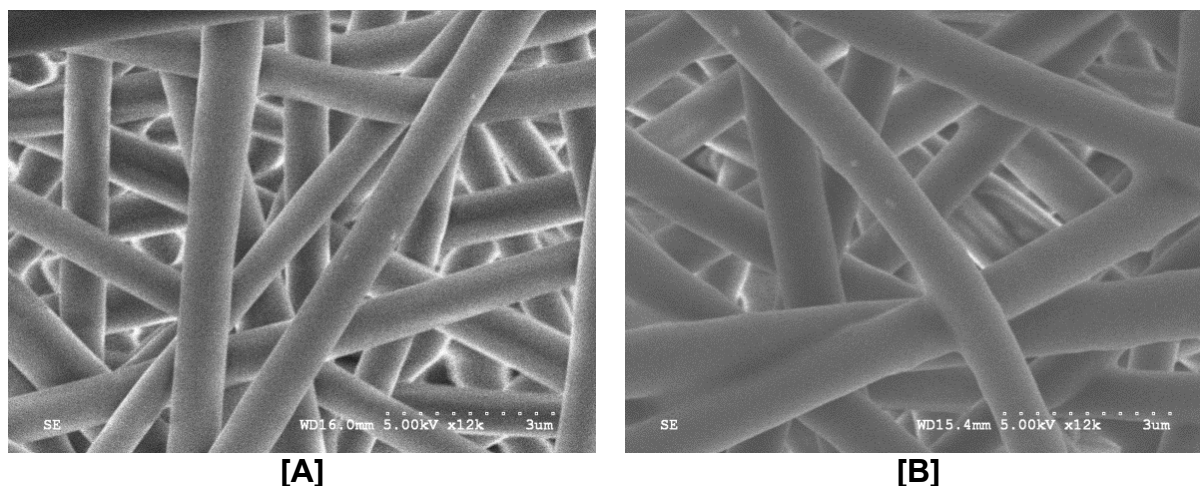


Figure 4. SEM images of lignin nanofiber mats before and after SI-ATRPase; [A] initiator-immobilized, SKL-Br (Diameter: 830 ± 81 nm), [B] Sample LPN-L-3 (Diameter: 1029 ± 116 nm) in **Table 1**.

The effect of reaction conditions on the enzymatic synthesis of PNIPAM on the lignin nanofibre surfaces.

To better understand the effect of the enzymes on PNIPAM brush synthesis, the enzymatic catalyzing activities of CBL, HRP and LTV were investigated by varying the concentration of reducing agent, and measuring the effect on the surface PNIPAM brush thickness (**Figure 5**). No PNIPMA brush formation was detected in the absence of the reducing reagents (AA or GL). Similarly, the use of glucose (GL) as the reducing reagent also did not produce any indication of PNIPAM brush synthesis in either the HRP or LTV systems. However, the CBL system did exhibit some catalytic activity, producing PNIPAM brushes with a thickness of about 25 ± 11 nm and a corresponding MW of 42.20×10^4 and PDI of 1.51. By contrast all of the catalytic systems were reactive in the presence of ascorbic acid (AA). At the same AA concentration, relatively low PNIPAM brush thickness was obtained with HRP compared to that of CBL and LTV (**Figure 5A**). The highest catalytic activity of HRP occurred at an AA concentration of 2.84×10^{-5} mol/L, resulting in a PNIPAM brush thickness of 53 ± 22 nm. However, further increasing the concentration of AA to 5.68×10^{-5} mol/L decreased the brush thickness to 10 ± 25 nm which was almost same as the one obtained at an AA concentration of 1.42×10^{-5} mol/L.

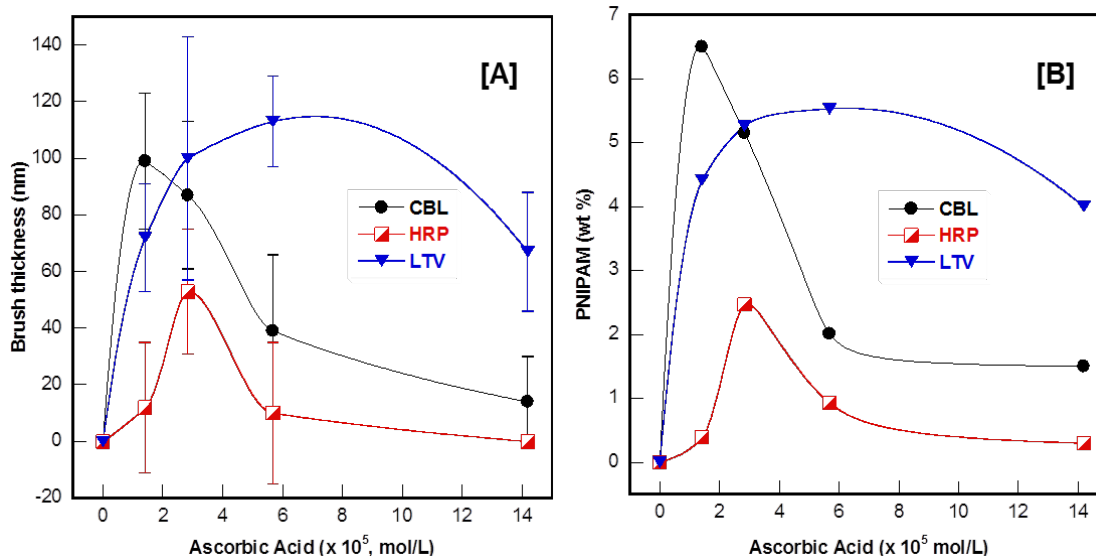


Figure 5. Quantitative analysis of PNIPAM brushes on lignin nanofiber mat. Comparison of the catalyzing activity of different enzymes [A] the effect of ascorbic acid concentration on PNIPAM brush thickness determined by SEM analysis [B] the effect of ascorbic acid concentration on the amount of PNIPAM (wt.%) grafted determined by DSC analysis.

A similar behavior was observed for CBL, which exhibited its highest activity at an AA concentration of 1.42×10^{-5} mol/L, with a corresponding PNIPAM brush thickness of 99 ± 24 nm. The catalyzing activity of CBL decreased gradually with increasing AA concentration producing PNIPAM brush thicknesses of about 14 ± 22 nm at an AA concentration of 14.18×10^{-5} mol/L. By contrast, the catalyzing activity of LTV showed a very different trend as compared to HRP and CBL. LTV activity gradually increased with increasing AA concentration from 1.42×10^{-5} to 5.68×10^{-5} mol/L, then decreased only slightly at 14.18×10^{-5} mol/L; the corresponding PNIPAM brush thicknesses increased from 72 ± 19 nm to 113 ± 16 nm, then decreased to 67 ± 21 nm, respectively. These results clearly demonstrate that the reducing reagent is dominating factor in the enzymatic synthesis of PNIPAM brushes on lignin nanofibre mat surfaces by ATRPase.

$$P\% = \frac{\Delta H_{LPN}}{\Delta H_p} \times M_N \times 100$$

1

$P\%$: PNIPAM weight percentage of LPN, ΔH_{LPN} : enthalpy of LPN sample (KJ/g), ΔH_p : enthalpy of per mole NIPAM ($= 6.28 \pm 0.18$ KJ/mol per NIPAM unit), M_N : molecular weight of NIPAM ($= 113.16$).

*Enthalpy analysis of PNIPAM immobilized onto lignin nanofibre mat surface*³⁷⁻⁴⁰

It has been shown that the enthalpy of transition (ΔH) of PNIPAM has a linear relationship with the quantity of NIPAM units.⁴¹ Therefore, we calculated the ΔH per NIPAM unit by using various concentrations of PNIPAM aqueous solution and obtained an $\Delta H = 6.28 \pm 0.18$ KJ/mol per NIPAM unit, which was within the range of published results (**Figure S1**).⁴¹⁻⁴⁴ The amount of surface grafted PNIPAM on the lignin nanofibres was related to ΔH by using **Equation 1**. **Figure 5B** shows the dependence of the amount of grafted PNIPAM (wt %) on AA concentration for the different enzymes (**Figure S2**). For all of the enzymes, the amount of grafted PNIPAM followed a very similar trend as PNIPAM brush thickness (see **Figure 5A**). Again, with no reducing agent (AA) in the reaction medium, no trace of PNIPAM was detected by ΔH analysis. Interestingly, the amount of PNIPAM calculated by ΔH analysis correlated well with the TGA results (*vide supra*). For example, the amount of PNIPAM grafted using LTV at an AA concentration of 2.84×10^{-5} mol/L (LPN-L-3) was calculated as ~ 5.3 wt %, which was close to the residual weight percentage for the same sample determined by TGA. Interestingly, the lignin nanofibre surface PNIPAM brush thickness is ~ 100 nm. It suggests that the PNIPAM brush was grafted on several surface layers of fibres of the lignin fibre mat, not on all of the lignin fibre. This is one of the unique characters of polymer brush surface grafting with enzyme as the catalyst in comparison with that of ATRP.⁹

Surface PNIPAM brush characterization.

To further analyze the enzymatic activity and the PNIPAM polymer brushes synthesized on the surface of the lignin nanofibre mats, the surface grafted PNIPAM was cleaved off by dissolving and extracting the lignin fiber at high aqueous NaOH concentrations wherein PNIPAM became insoluble.⁹ The chemical structure of the cleaved PNIPAM from the nanofibre mat surface was confirmed by ^1H and ^{13}C NMR (**Figure 6**) and GPC analysis (**Figure 7**), and is summarized in **Table 1**.

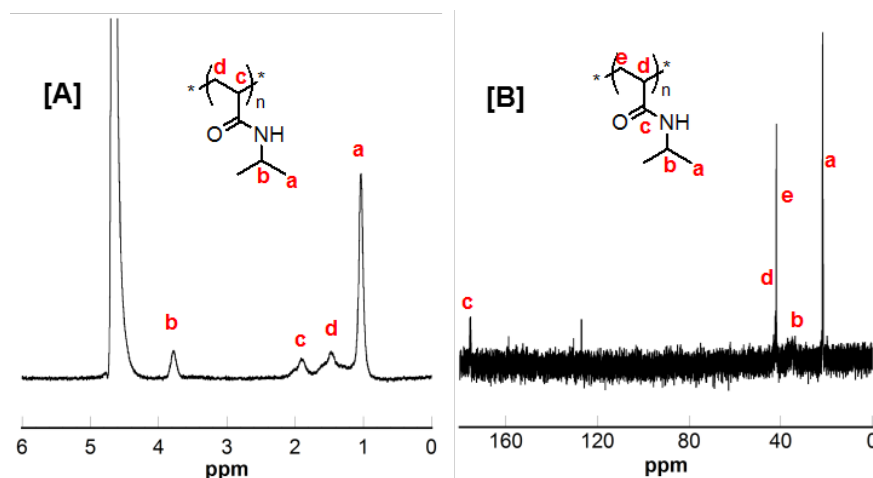
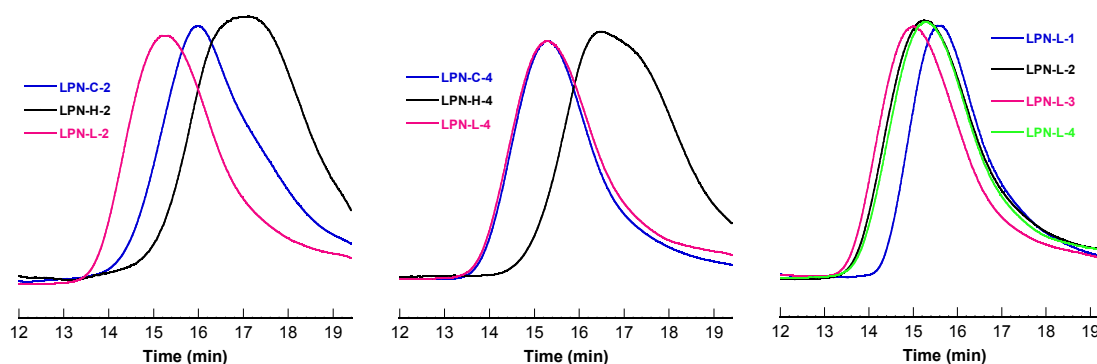


Figure 6. ^1H NMR [A] and ^{13}C NMR [B] spectra of PNIPAM brushes cleaved from the lignin nanofibre mat surfaces.

The GPC curves of the LTV and CBL catalyzed systems appeared monomodal, while those of the HRP catalyzed systems were relatively broad, with lower molecular weight shoulders present at lower ascorbic acid concentration (**Figure 7**). The PDI of the LTV catalyzed PNIPAM brushes produced in pure water ranged between 1.23 - 1.40, suggesting the living polymerization of NIPAM on the surface of the lignin nanofibre mats. By contrast the CBL and HPL catalyzed system were slightly higher at 1.31 - 1.53 and 1.66 - 2.93, respectively. Moreover, when the reactions were run in PBS at pH 6 (AA concentration of 5.68×10^{-5} mol/L) the PDI was ~ 1.50 for both the LTV and HRP, implying poorer control in the LTV, but better control in the HRP system, respectively.



In fact, there was no significant difference in the PNIPAM grafting densities between all of the three enzyme systems using AA as the reducing reagent in water; grafting densities ranged from 7.3×10^{-2} to 12.39×10^{-2} chains/nm². In the case of glucose and the CBL catalyst, the PNIPAM density dropped to 3.96×10^{-2} chains/nm², with no trace of PNIPAM brushes found in the HRP and LTV systems.

Stimuli-response of PNIPAM grafted lignin nanofiber.

PNIPAM in aqueous solutions has a phase transition with a lower critical solution temperature (LCST) of ~ 32 °C, and is dependent on ionic concentration.^{45,46} **Figure 8** shows the effect of sodium sulfate concentration on the LCST of LPN-L-3. The slope of the LCST exhibited two trends, i.e. the slope between concentrations from 0 – 0.1 M was larger than that from 0.2 – 0.5 M. The LCST of PNIPAM grafted lignin nanofibre mats was 26.3 °C at a salt concentration of 0.1 M. It gradually decreased to 23.4 and 14.7 °C when the salt concentration increased from 0.2 to 0.5 M, suggesting that the PNIPAM modified lignin nanofibre mat surface became hydrophobic when the salt concentration was higher than 0.2 M at room temperature.

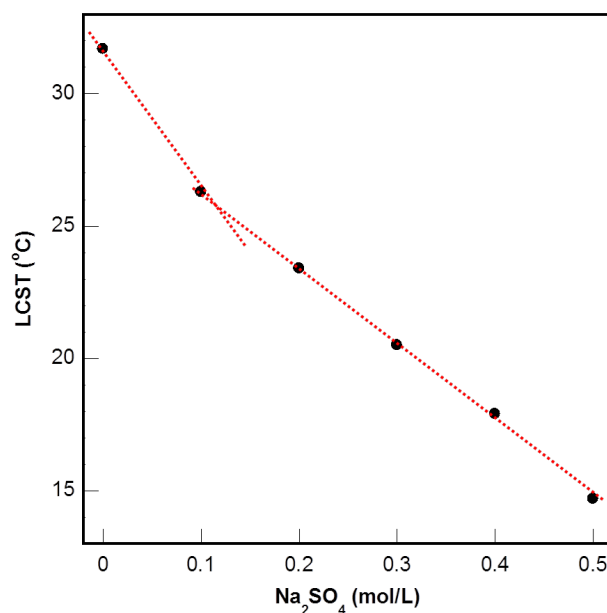


Figure 8. Effect of salt concentration on the lower critical solution temperature (LCST) of PNIPAM brush grafted lignin nanofibre mats (sample LPN-L-3 in **Table 1**).

Water contact angle experiments were performed and the findings correlated very well with the LCST analysis (**Figure 9**). The water contact angles of PNIPAM grafted lignin nanofiber mats decreased very fast when the salt concentration was lower than 0.1 M, and became 0° in ~40 s and 80 s at salt concentrations of 0.0 and 0.1 M, respectively. However, the water contact angles of the PNIPAM immobilized lignin nanofiber mats was still ~70° at a salt concentration of 0.2 M after 120 s, and became completely hydrophobic at salt concentrations of 0.4 and 0.5 M, where the water contact angles stabilized at ~120°. Under these conditions, the surface-grafted PNIPAM brushes are suggested to have a globular contracted chain form.

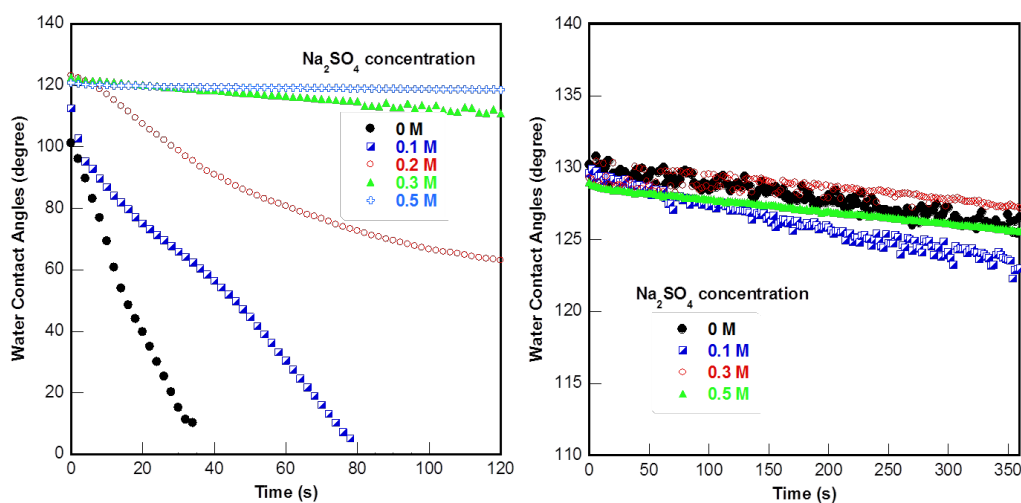


Figure 9. Effect of salt concentration on water contact angles of lignin nanofiber mats. **[A]** Time dependent water contact angles of LPN at various Na_2SO_4 concentrations. **[B]** Control sample: Time dependent water contact angles of Lignin-Br at various Na_2SO_4 concentrations.

Conclusion:

Lignin nanofibre mats were successfully modified with PNIPAM brushes for the first time through a SI-ATRPase mechanism in aqueous medium at room temperature. ATR-FTIR, TGA, XPS, SEM and water contact angle measurements confirmed that all of three enzymes investigated, CBL, HRP, and LTV had catalytic activity for PNIPAM brush immobilization on the surface of lignin nanofibres. Analysis of the PNIPAM brushes cleaved from the surface of

the lignin nanofibre mats by NMR and GPC showed low PDI with CBL and LTV catalysts, indicating the characteristics of living radical polymerization. PNIPAM brushes with various molecular weights were obtained by controlling reaction conditions, such as the type of enzyme, the concentration of reducing reagent and solution pH. Surface PNIPAM brush thickness was determined by SEM analysis and found to show similar trends with respect to enzyme activity as the weight percentage of surface PNIPAM calculated from DSC (enthalpy of transition) analysis. Lignin nanofiber mats modified with PNIPAM exhibited ionic-responsive and temperature-sensitive characteristics and had a similar LCST as the pure PNIPAM. These results indicate that enzyme-catalyzed SI-ATRP can build a new platform for the living controllable surface functional polymer brush modification of biopolymer nanofibres.

References

1. Holladay, J. E., J. F. White, J. J. Bozell and D. Johnson “Top Value-Added Chemicals from Biomass Volume II—Results of Screening for Potential Candidates from Biorefinery Lignin” **2007**, DOE.
2. Kadla, J. F.; Kubo, S.; Gilbert, R. D.; Venditti, R. A.; Compere, A.; Griffith, W. *Carbon* **2002**, *40*, 2913 – 2920.
3. Kubo, S.; Gilbert, R. D.; Kadla, J. F. Lignin-based polymer blends and biocomposite materials. In *Natural Fibers, Biopolymers, and Biocomposites*; Mohanty, A., Misra, M., Drzal, L., Eds.; Oxford Press: New York, **2005**; pp 671 – 697.
4. Dallmeyer, I.; Ko, F.; Kadla, J. F. *J. Wood Chem. Technol.* **2010**, *30*, 315 – 329.
5. Kadla, J. F.; Kubo, S.; Venditti, R. A.; Gilbert, R. D. *J. Appl. Polym. Sci.* **2002**, *85*, 1353 – 1355.
6. Dallmeyer, I.; Chowdhury, S.; Kadla, J. F. *Biomacromolecules* **2013**, *14*, 2354 – 2363.
7. Teng, N.-Y.; Dallmeyer, I.; Kadla, J. F. *Ind. Eng. Chem. Res.* **2013**, *52*, 6311 – 6317.
8. Kim, Y. S.; Kadla, J. F. *Biomacromolecules* **2010**, *11*, 981 – 988.
9. Gao, G.; Dallmeyer, J. I.; Kadla, J. F. *Biomacromolecules* **2012**, *13*, 3602 – 3610.
10. Zhao, B.; Brittain, W.J. *Prog. Polym. Sci.* **2000**, *25*, 677 – 710.
11. Edmondson, S.; Osborne, V. L.; Huck, W. T. S. *Chem. Soc. Rev.* **2004**, *33*, 14 – 22.
12. Hong, C.-Y.; You, Y.-Z.; Pan, C.-Y. *Chem. Mater.* **2005**, *17*, 2247 – 2254.

13. Takei, Y. G.; Aoki, T.; Sanui, K.; Ogata, N.; Sakurai, Y.; Okano, T. *Macromolecules* **1994**, *27*, 6163 – 6166.
14. Osada, Y.; Honda, K.; Ohta, M. *J. Membrane Sci.* **1986**, *27*, 327-338.
15. Park, Y. S.; Ito, Y.; Imanishi, Y. *Langmuir* **1998**, *14*, 910-914.
16. Abu-Lail, N. I.; Kaholek, M.; LaMattina, B.; Clark, R. L.; Zauscher, S. *Sensor Actuat B-Chem.* **2006**, *114*, 371-378.
17. Yamato, M.; Konno, C.; Utsumi, M.; Kikuchi, A.; Okano, T. *Biomaterial* **2002**, *23*, 561-567.
18. Yoshioka, H.; Mikami, M.; Nakai, T.; Mori, Y. *Polym Advan Technol* **1995**, *6*, 418-420.
19. Cunliffe, D.; Alarcon, C. D.; Peters, V.; Smith, J. R.; Alexander, C. *Langmuir* **2003**, *19*, 2888-2899.
20. Okano, T.; Kikuchi, A.; Sakurai, Y.; Takei, Y.; Ogata, N. *J Control Release* **1995**, *36*, 125-133.
21. Akiyama, Y.; Kikuchi, A.; Yamato, M.; Okano, T. *Langmuir* **2004**, *20*, 5506-5511.
22. Duracher, D.; Elaissari, A.; Mallet, F.; Pichot, C. *Langmuir* **2000**, *16*, 9002-9008.
23. Ionov, L.; Stamm, M.; Diez, S. *Nano Lett* **2006**, *6*, 1982-1987.
24. Taniguchi, T.; Duracher, D.; Delair, T.; Elaissari, A.; Pichot, C. *Colloid Surface B* **2003**, *29*, 53-65.
25. Bromberg, L. E.; Ron, E. S. *Adv Drug Deliver Rev* **1998**, *31*, 197-221.
26. Bergbreiter, D. E.; Caraway, J. W. *J Am Chem Soc* **1996**, *118*, 6092-6093.
27. Bergbreiter, D. E.; Koshti, N.; Franchina, J. G.; Frels, J. D. *Angew Chem Int Edit* **2000**, *39*, 1040-1045.
28. Chen, G. H.; Hoffman, A. S. *Nature* **1995**, *373*, 49-52.
29. Hong, C. Y.; You, Y. Z.; Pan, C. Y. *Chem Mater* **2005**, *17*, 2247-2254.
30. Sun, T. L.; Wang, G. J.; Feng, L.; Liu, B. Q.; Ma, Y. M.; Jiang, L.; Zhu, D. B. *Angew Chem Int Edit* **2004**, *43*, 357-3.
31. Pyun, J.; Kowalewski, T.; Matyjaszewski, K. *Macromol. Rapid Commun.* **2003**, *24*, 1043 – 1059.
32. Kobayashi, S.; Makino, A. *Chem. Rev.* **2009**, *109*, 5288 –5353.
33. Sigg, S. J.; Seidi, F.; Renggli, K.; Silva, T. B.; Kali, G.; Bruns, N. *Macromol. Rapid Commun.* **2011**, *32*, 1710 – 1715.

34. Ng, Y.-H.; Lenaz, F. d.; Chai, C. L. L. *Chem. Commun.* **2011**, *47*, 6464 – 6466.
35. Ng, Y.-H.; Lenaz, F. d.; Chai, C. L. L. *Polym. Chem.* **2011**, *2*, 589 – 594.
36. Yamashita, K.; Yamamoto, K.; Kadokawa, J. *Polymer* **2013**, *54*, 1775 – 1778.
37. Qiu, X-P.; Koga, T.; Tanaka, F.; Winnik, F. M. *Sci. China Chem.* **2013**, *56 (1)*, 56 – 64.
38. Tiktopulo, E. I.; Bychkova, V. E.; Ricka, J.; Ptitsyn, O. B. *Macromolecules* **1994**, *27*, 2879 – 2882.
39. Kujawa, P.; Winnik, F. M. *Macromolecules* **2001**, *34*, 4130 – 4135.
40. Avoce, D.; Liu, H. Y.; Zhu, X. X. *Polymer* **2003**, *44*, 1081 – 1087.
41. Qiu, X-P.; Koga, T.; Tanaka, F.; Winnik, F. M. *Sci. China Chem.* **2013**, *56 (1)*, 56 – 64.
42. Tiktopulo, E. I.; Bychkova, V. E.; Ricka, J.; Ptitsyn, O. B. *Macromolecules* **1994**, *27*, 2879 – 2882.
43. Kujawa, P.; Winnik, F. M. *Macromolecules* **2001**, *34*, 4130 – 4135.
44. Avoce, D.; Liu, H. Y.; Zhu, X. X. *Polymer* **2003**, *44*, 1081 – 1087.
45. Zhang, Y. J.; Furyk, S.; Bergbreiter, D. E.; Cremer, P. S. *J. Am. Chem. Soc.* **2005**, *127*, 14505 – 14510.
46. Fu, H.; Hong, X. T.; Wan, A.; Batteas, J. D.; Bergbreiter, D. E. *ACS Appl. Mater. Interfaces* **2010**, *2*, 452 – 458.